International Journal of Solids and Structures 52 (2015) 45–55

Contents lists available at ScienceDirect

International Journal of Solids and Structures

journal homepage: www.elsevier.com/locate/ijsolstr

A gradient approach for the macroscopic modeling of superelasticity in softening shape memory alloys

A.A. León Baldelli [a], C. Maurini [b,c], K. Pham [d,*]

[a] Center for Computation & Technology, Louisiana State University, USA
[b] Institut Jean Le Rond d'Alembert, UPMC Univ Paris 06 (UMR 7190), 4 place Jussieu, 75252 Paris, France
[c] Institut Jean Le Rond d'Alembert, CNRS (UMR 7190), 4 place Jussieu, 75252 Paris, France
[d] Unité de Mécanique, ENSTA ParisTech, Chemin de la Hunière et des Joncherettes, 91761 Palaiseau Cedex, France

ARTICLE INFO

Article history:
Received 24 July 2014
Received in revised form 11 September 2014
Available online 6 October 2014

Keywords:
Shape memory alloys (SMA)
Superelasticity
Softening
One dimensional model
Energetic approach
Regularization

ABSTRACT

This paper presents a gradient approach for the quasi-static macroscopic modeling of superelasticity in softening shape memory alloys bars. The model is assumed to be rate-independent and to depend on a single internal variable. Regularization of the model is achieved through the free energy by assuming a quadratic dependance with respect to the gradient of the internal variable. The quasi-static evolution is then formulated in terms of two physical principles: a stability criterion which consists in selecting the local minima of the total energy of the system and an energy balance condition. Both homogeneous and non-homogeneous evolutions are investigated analytically for a family of material parameters. Non-homogeneous evolutions can be divided into three stages: the localized martensite nucleation followed by the propagation of the localized phase transformation front and finally the annihilation of the austenite phase. For each stage, the local phase field profile as well as the global stress–strain response are derived in closed-form. Due to the presence of an internal length related to the regularization, size effects are inherent with such non-local model. We show that for sufficiently long bars, snap-backs occur at the onset of localized phase transformation, leading to a time discontinuity in the quasi-static evolution.

1. Introduction

Quasi-static tensile tests performed on superelastic NiTi strips or wires at various speeds show that the martensitic phase transformation is a *non-homogeneous* process (Huo and Müller, 1993; Shaw and Kyriakides, 1995, 1997; Tobushi et al., 1993). It is characterized in the global response by a first elastic-hardening phase followed by a macroscopic instability: depending on the loading rate, one or several martensite localizations nucleate along the specimen and propagate at constant stress. Due to such non-homogeneous response, the extraction of the intrinsic response of SMA by means of a tensile test is a difficult task. Such underlying material response is nevertheless fundamental for an appropriate calibration of the macroscopic constitutive SMA models. Recently, Hallai and Kyriakides (2013) have been able to stabilize a homogeneous phase transformation in the case of a superelastic NiTi. By bonding stainless steel to the NiTi strip, instabilities in the NiTi specimen are avoided due to the hardening character of the stainless steel, thus leading to a *homogeneous* phase transformation. By subtracting the response of the stainless steel from the response of the bonded specimen, extraction of the (forward) intrinsic macroscopic behavior of the NiTi is then achieved. Stress–strain response during the phase transformation is non-monotonous, showing a significant softening part. Such result is consistent with the fact that the critical stress at which occurs the non-homogeneous phase transformation of NiTi corresponds approximatively to the Maxwell line associated to the softening intrinsic curve. Such experimental evidences emphasize the necessity to account for the softening behavior in the macroscopic modeling of SMAs in order to provide a correct modeling of their structural behavior and a better understanding of the localization phenomena (Song et al., 2012; Pham, 2014).

An important class of macroscopic superelastic SMA models for superelasticity is based on the description of the phase transformation by means of internal variables. Such models can be either derived from a micro-mechanical approach (Sun and Hwang, 1993a,b; Cherkaoui et al., 1998) or established phenomenologically by postulating the free energy as well as the dissipated potential with respect to the laws of thermodynamics (Auricchio and Sacco, 1997; Popov and Lagoudas, 2007; Zaki and Moumni, 2007; Song et al., 2012; Pham, 2014). However, most of these studies

* Corresponding author.
E-mail address: kim.pham@ensta-paristech.fr (K. Pham).

http://dx.doi.org/10.1016/j.ijsolstr.2014.09.009
0020-7683/

remain *local* in the sense that the constitutive behavior at a given point in space is function of the state variables of the same point only, being independent of the gradient of the state variables or of the state of other points. Such local approach is valid as long as the behavior does not show any sign of stress softening. As soon as the intrinsic behavior exhibits stress softening, local models are not any more mathematically well-posed and show a number of serious pathologies. In particular, an infinite number of austenite–martensite macroscopic interfaces can nucleate without any energy dissipation. This is in contradiction with the experimental results for which the number of localization is limited to one or two for very slow loading rate. From the numerical point of view, strong mesh sensitivities are observed and the propagation of the phase transformation cannot be handled correctly. To avoid such issues regularized models of SMA models must be considered. Following the seminal work of Ericksen (1975), this has been mainly done in the context of SMA by introducing either the gradient of the strain (Carr et al., 1985; Friedman and Sprekels, 1990; Shaw, 2002) or the gradient of the internal variable (Duval et al., 2011) in the constitutive equations and phase transformation criteria. Some of these works exhibit numerical examples illustrating the benefit of the regularization during the non-homogeneous phase transformation. However analytical and rigorous results are not always available on the properties of the localized solutions and their evolution. Such results are fundamental to better understand the impact of the regularization on the model behavior.

In this paper we consider a regularized model for a SMA bar with stress-softening regularized through the introduction of an internal length and an energy dissipation depending on the gradient of the phase-field. We derive a fully analytical solution of the one-dimensional evolution problem including explicit expressions for the homogeneous and localized response and a full description of the nucleation phase and the propagation of the phase-transformation front. Moreover we show that global strain–stress response can exhibit a snap-back depending on the ratio between the length of the bar and the introduced internal length. The regularization introduces a scale-effect, as classical in damage and fracture (Bazant and Pijaudier-Cabot, 1989; Pham et al., 2011). Our model is formulated in the framework of the variational theory of rate-independent standard processes (Halphen and Nguyen, 1975; Mielke, 2005). The cornerstone of this framework is the minimization (in a certain sense) of the total energy of the system. Such minimizing technique proves to be a particularly powerful tool for non-convex problems such as phase transformation, plasticity or fracture. Although it has been widely used at the microscopic scale to account for the formation of martensite domains, self-accommodation as well as shape-memory effect (Ball and James, 1989; Puglisi and Truskinovsky, 2000; Ren and Truskinovsky, 2000; Bhattacharya, 2003), such minimization approach can be also extended to macroscopic scale to deal with the evolution of stress-softening SMAs. In our context, the quasi-static evolution is required to verify a local stability criterion and an energy balance condition, requiring the continuity of the total energy with respect to the loading parameter. This framework has proved its efficiency in many areas which involve stress-softening issues such as brittle fracture (Bourdin et al., 2008), damage (Pham et al., 2011), or coupled damage-plasticity (Alessi et al., 2014). This work can be regarded as an extension of Pham (2014), where a local SMA model is formulated and analyzed in the same framework.

The paper is organized as follows. In Section 2, we introduce the energetic formulation of the one dimensional non-local superelastic model of SMA with gradient of the phase transformation variable. Section 3 presents the study of a one dimensional bar submitted to a tensile test. The associated evolution problem is formulated in terms of a stability criterion based on the selection of *local* minima of the total energy and an energy balance. The strong formulation in terms of Kuhn–Tucker conditions is then derived under specific hypothesis. In Section 4, we present the homogeneous evolution of the bar and calibrate our model according to published experimental data. Section 5 is devoted to the analysis of solution involving the localization of the phase field. The localization profile as well as the associated global stress–strain response are derived for a class of material functions and discussed. Conclusions are drawn in Section 6.

The following notations are used: the dependence on the time parameter t is indicated by a subscript whereas the dependence on the spatial coordinate x is indicated classically by parentheses, *e.g.* $x \mapsto u_t(x)$ stands for the displacement field at time t. In general, the material functions of the phase transformation variable are represented by sans serif letters, like E, G or R. The prime denotes either the derivative with respect to x or the derivative with respect to the phase transformation variable, the dot stands for the time derivative, *e.g.* $u_t'(x) = \partial u_t(x)/\partial x$, $\mathsf{E}'(\alpha) = d\mathsf{E}(\alpha)/d\alpha$ or $\dot{u}_t(x) = \partial u_t(x)/\partial t$.

2. Gradient model of SMA with an internal variable

Macroscopic phase transformation processes are usually understood as rate-independent processes. The main source of rate-dependency usually comes from the heat release during the austenitic–martensitic phase transformation which has an autocatalytic effect. However, by enforcing sufficiently slow elongation rate ($\sim 10^{-5}\,\mathrm{s}^{-1}$ to $10^{-4}\,\mathrm{s}^{-1}$), the system can be considered as isothermal and fully rate-independent. Such quasi-static hypothesis will be considered in this article. The modeling of the macroscopic superelastic behavior of SMA will be done within the *standard* framework (Halphen and Nguyen, 1975) for which the material behavior admits an energetic formulation. The standard model we will consider is based on a single scalar internal variable z which will account both for the phase transformation as well as the transformation strain due to the oriented martensite (Pham, 2014). We assume that z belongs to the interval $[0,1]$, with $z = 0$ and $z = 1$ representing a fully transformed state of austenite and martensite, respectively. The formulation of the standard model starts here by postulating directly the form of the strain work density at a material point. In a non-local setting, we assume that this material point is described by its strain state ε, the phase field z and its gradient z'. Hence, let us call $W(\varepsilon, z, z')$ the strain work required to transform a material point from the reference state $(0,0,0)$ to a state (ε, z, z'). This quantity depends not only on the final state (ε, z, z') but also on the history of the loading because of the dissipative nature of the transformation. For standard models of dissipative processes and for *homogeneous* evolutions (no effect of gradient *i.e.* $z' = 0$), the strain work can be decomposed as follows

$$W(\varepsilon, z, 0) = \phi(\varepsilon, z) + \mathcal{D}(z, \dot{z}), \tag{1}$$

where $\phi(\varepsilon, z)$ and $\mathcal{D}(z, \dot{z})$ represent the local free energy and the total dissipated energy, respectively. Under the small strain assumption, the free energy is taken as a quadratic function of ε which is cast under the following form

$$\phi(\varepsilon, z) = \frac{1}{2}\mathsf{E}(z)(\varepsilon - \mathsf{p}(z))^2 + \mathsf{G}(z). \tag{2}$$

The free energy is a *state function* which does not depend on the history of the loading and which involves four material functions of the internal variables, namely the Young's modulus of the mixture of austenite–martensite $z \mapsto \mathsf{E}(z)$, the phase transformation strain $z \mapsto \mathsf{p}(z)$ and the latent energy released (or absorbed) during the forward (or the backward) phase transformation $z \mapsto \mathsf{G}(z)$. For the following developments it is useful to introduce also the compliance function $\mathsf{S} : z \mapsto 1/\mathsf{E}(z)$. The total dissipated energy $\mathcal{D}(z, \dot{z})$ depends on the history of the loading. For rate-independent processes, its time derivative, the intrinsic dissipation, is a homogeneously positive function of degree 1 of $\dot{z}$. As a result, $\mathcal{D}(z,\dot{z})$ can be written as

$$\mathcal{D}(z,\dot{z}) = \int_0^t \mathsf{R}'(z)|\dot{z}|d\tau, \qquad (3)$$

where $\mathsf{R}(z)$ is a material function such that $\mathsf{R}(0)=0$. In virtue of the second law of thermodynamics which stipulates that the rate of dissipation $\dot{\mathcal{D}}(z,\dot{z}) = \mathsf{R}'(z)|\dot{z}|$ is positive, we have necessarily $\mathsf{R}'>0$. The quantity $\mathsf{R}(z)$ can be interpreted as the total dissipated energy during a *monotonous* forward phase transformation from 0 to z such that $\dot{z}>0$. To provide a correct response of the model at the local level, we make the following assumptions:

Hypothesis 2.1. We assume that all the material functions are differentiable and we suppose

- $\mathsf{E}'>0$ with $\mathsf{E}(0)=\mathsf{E}_\mathsf{A}$ and $\mathsf{E}(1)=\mathsf{E}_\mathsf{M}$;
- $\mathsf{p}'>0$ with $\mathsf{p}(0)=0$ and $\mathsf{p}(1)=\mathsf{p}_1$;
- $\mathsf{R}'>0$ with $\mathsf{R}(0)=0$ and $\mathsf{R}(1)=\mathsf{R}_1$;
- $\mathsf{G}'-\mathsf{R}'>0$ with $\mathsf{G}(0)=0$.

The parameters E_A (*resp.* S_A) and E_M (*resp.* S_M) represent the Young's modulus (*resp.* the compliance) of the austenite and the martensite phases respectively with $\mathsf{E}_\mathsf{A}>\mathsf{E}_\mathsf{M}; \mathsf{p}_1>0$ is the maximum martensite strain reached at the end of the phase transformation; $\mathsf{R}_1>0$ is the total energy dissipated during a monotonous austenite to martensite transformation. As a result, the assumptions on the monotonicity of E,p and R follow from the physical meaning of $\mathsf{E}_\mathsf{A},\ \mathsf{E}_\mathsf{M},\ \mathsf{R}_1$ and p_1. An energetic explanation on the assumption $\mathsf{G}'-\mathsf{R}'>0$ will be given once the evolution problem is obtained.

To penalize the nucleation of localized interfaces at the macroscopic scale, we choose here to introduce gradient effects in the standard model by assuming that the free energy of a state (ε,z,z') is, as done in gradient damage models (Frémond and Nedjar, 1996; Pham et al., 2011), a function of not only the local variables (ε,z) but also of the spatial gradient of the phase transformation variable z'. In a linearized setting, the non-local strain work then reads

$$W(\varepsilon,z,z') = \frac{1}{2}\mathsf{R}_1\ell^2 z'^2 + \phi(\varepsilon,z) + \int_0^t \mathsf{R}'(z)|\dot{z}|d\tau, \qquad (4)$$

where the term involving the gradient of z has to be positive to effectively penalize interfaces. As a result, by renormalizing the gradient term by R_1, the non-local term introduces an internal length ℓ which is an additional material parameter to be identified. Other choices can be considered such as introducing gradient effects into the dissipated energy density (3) as done in gradient model of crystal plasticity (Gurtin and Anand, 2005; Qiao et al., 2011).

3. Evolution problem

3.1. Energetic formulation of the evolution problem

We consider a one dimensional SMA bar of length L and axial coordinate $x\in[0,L]$ whose displacements are prescribed at the extremities of the bar. The end $x=0$ of the bar is fixed, whereas the displacement of the end $x=L$ is submitted to a value U_t depending on an increasing parameter t which plays the role of the "time". The nominal strain is then given by $\bar{\varepsilon}_t = U_t/L$. For this one dimensional problem, the admissible displacement fields and phase-field belongs to the following spaces

$$\mathcal{C}_t = \{u\in H^1(0,L) : u(0)=0, u(L)=U_t\}, \quad \mathcal{Z}_0 = H^1((0,L),[0,1]), \qquad (5)$$

where $H^1(0,L)$ is the space of functions that are square integrable and whose first derivatives are square integrable while $H^1((0,L),[0,1])$ is the closed subspace of functions of $H^1(0,L)$ bounded by 0 and 1. For a given $z\in\mathcal{Z}_0$, let us associate the space of admissible test directions $\mathcal{Z}(z)$ defined by

$$\mathcal{Z}(z) = \{\beta\in H^1(0,L) : \beta\geqslant 0 \text{ where } z=0, \quad \beta\leqslant 0 \text{ where } z=1\}. \qquad (6)$$

For an admissible state of displacement and phase transformation variable $(u_t,z_t)\in\mathcal{C}_t\times\mathcal{Z}_0$, the total energy of the system in this state reads

$$\mathcal{P}_t(u_t,z_t) = \int_0^L W(u_t',z_t,z_t')dx = \mathcal{E}(u_t,z_t) + \int_0^L\int_0^t \mathsf{R}'(z_\tau)\mid\dot{z}_\tau\mid d\tau dx, \qquad (7)$$

where the total free energy is given by

$$\mathcal{E}(u_t,z_t) = \int_0^L \left(\frac{1}{2}\mathsf{R}_1\ell^2 z_t'^2 + \phi(u_t',z_t)\right)dx. \qquad (8)$$

A variational formulation of the evolution problem allows the natural derivation of the evolution equations including the role of the gradient term. Specifically, we require the solutions of the evolution problem to obey two basic principles, namely a stability criterion (**S**) and an energy balance condition (**E**):

$$(\mathbf{S}):\quad \begin{cases} \forall(v,\beta)\in\mathcal{C}_0\times\mathcal{Z}(z_t), \exists r^*>0, \forall h\in[0,r^*), (u_t+hv, z_t+h\beta)\in\mathcal{C}_t\times\mathcal{Z}_0, \\ \mathcal{P}_t(u_t,z_t)\leqslant \mathcal{E}(u_t+hv,z_t+h\beta) + \int_0^L\int_0^t \mathsf{R}'(z_\tau)\mid\dot{z}_\tau\mid d\tau dx + \int_0^L \mid\mathsf{R}(z_t+h\beta)-\mathsf{R}(z_t)\mid dx, \end{cases} \qquad (9)$$

$$(\mathbf{E}):\quad \mathcal{P}_t(u_t,z_t) = \mathcal{P}_0(u_0,z_0) + \int_0^t \sigma_{t^*}\dot{U}_{t^*}dt^*. \qquad (10)$$

The stability criterion consists in selecting local minimizers of the total energy among all the possible admissible states at each time step. Indeed, the right-hand side of (**S**) can be interpreted as the total energy of the state $(u_t+hv,z_t+h\beta)$ obtained as the final state of an infinitesimal evolution from the state (u_t,z_t) in the direction $(hv,h\beta)$. In particular the term $\int_0^L\mid\mathsf{R}(z_t+h\beta)-\mathsf{R}(z_t)\mid dx$ represents the total dissipated energy to evolve from z_t to $z_t+h\beta$ along a monotonic evolution. This stability criterion allows to select physically observable solutions. This is particularly important when uniqueness is no longer guaranteed, as typical in softening models including bifurcation and localization phenomena.

The energy balance condition requires the absolute time continuity of the total energy with respect to the time. While this condition gives the classical Kuhn–Tucker consistency condition for evolutions regular in time, this global condition can be used to follow also brutal evolutions. As we will see in Section 5.2, this happens in case of snap-back in the global response.

To make the link with the classical formulations of phase transformations which usually performed at the local level, let us derive the first order conditions of optimality of this problem.

3.2. Strong formulation of the problem

The strong formulation of the evolution problem is obtained by establishing the first order optimality condition which is a necessary condition of local minimality. Starting from (9), this condition reads

$$\forall(v,\beta)\in\mathcal{C}_0\times\mathcal{Z}(z_t),\quad \lim_{h\to 0}\frac{\mathcal{E}(u_t,z_t)-\mathcal{E}(u_t+hv,z_t+h\beta)}{h} \leqslant \lim_{h\to 0}\frac{\int_0^L \mid \mathrm{R}(z_t+h\beta)-\mathrm{R}(z_t)\mid dx}{h}. \quad (11)$$

Taking the limit when h tends to 0, we obtain

$$-D\mathcal{E}_t(u_t,z_t)(v,\beta)\leqslant\int_\Omega \mathrm{R}'(z_t)\mid\beta\mid dx, \quad (12)$$

which conversely reads

$$\int_0^L\left(\frac{\partial\phi}{\partial\varepsilon}(u_t',z_t)\,v'+\frac{\partial\phi}{\partial z}(u_t',z_t)\beta+\mathrm{R}_1\ell^2 z_t'\beta'+\mathrm{R}'(z_t)|\beta|\right)dx\geqslant 0. \quad (13)$$

Such variational formulation leads to the strong formulation of the mechanical equilibrium as well as the phase transformation criteria. In particular we have the following result (the proof is reported in Appendix A):

Proposition 3.1 (Phase transformation criteria). *In* $(0,L)$*, the phase transformation criteria are the following:*

$$\frac{\partial\phi}{\partial z}(u_t',z_t)-\mathrm{R}_1\ell^2 z_t''+\mathrm{R}'(z_t)\geqslant 0\quad\text{where}\quad z_t<1, \quad (14)$$

$$-\frac{\partial\phi}{\partial z}(u_t',z_t)+\mathrm{R}_1\ell^2 z_t''+\mathrm{R}'(z_t)\geqslant 0\quad\text{where}\quad z_t>0. \quad (15)$$

At the boundaries, we have at $x=0$

$$z_t'(0)\geqslant 0\quad\text{if}\quad z_t(0)<1,\qquad z_t'(0)\leqslant 0\quad\text{if}\quad z_t(0)>0 \quad (16)$$

and at $x=L$

$$z_t'(L)\leqslant 0\quad\text{if}\quad z_t(L)<1,\qquad z_t'(L)\geqslant 0\quad\text{if}\quad z_t(L)>0. \quad (17)$$

The derivation of the consistency conditions at the local level is obtained from the energy balance conditions. Here, we assume that the evolution fields are regular enough in time so that the derivative in time of the phase transformation field makes sense. Specifically, by taking the derivative in time of (10) and after some calculations which are reported in Appendix A, we obtain the following result.

Proposition 3.2 (Phase transformation consistency condition). *In* $(0,L)$*, the phase transformation consistency condition is the following:*

$$\mathrm{R}'(z_t)\dot{z}_t=\left(-\frac{\partial\phi}{\partial z}(u_t',z_t)+\mathrm{R}_1\ell^2 z_t''\right)|\dot{z}_t|. \quad (18)$$

At the boundaries, we have

$$z_t'(L)\dot{z}_t(L)=0,\quad z_t'(0)\dot{z}_t(0)=0. \quad (19)$$

Therefore, the Kuhn–Tucker conditions of the phase transformation including the non-local contributions are obtained as a first order condition of optimality associated to the stability criterion in combination with the energy balance condition written for regular solutions in time.

4. Homogeneous evolution

4.1. Stress–strain response

Homogeneous evolutions are of particular interest from the experimental point of view as they give a direct access to the intrinsic behavior of the material. They consist in evolutions for which both the strain and the phase transformation variable do not depend on x. The strain field is then equal to the average (nominal) strain $\bar{\varepsilon}_t$. For such homogeneous behavior, the mechanical equilibrium (71) is automatically satisfied and it remains to investigate the phase transformation evolution. One has to solve the Kuhn–Tucker conditions (75), (77) and (84) with null gradient terms.

This problem has been studied in Pham (2014). We report in the following Propositions the main results obtained for the homogenous forward and backward phase transformation at *prescribed strain*

Proposition 4.1 (Homogeneous forward phase transformation). *The response of the material point during the loading phase* ($t\mapsto\bar{\varepsilon}_t$ *increasing) follows three successive stages:*

1. *Austenite phase:* $\bar{\varepsilon}_t\in[0,\bar{\varepsilon}_{\mathrm{AM}}(0)]$. *At the onset of the loading, the response of the material is first elastic. The phase transformation variable is equal to 0 and the stress–strain relation reads*

$$\sigma_t=\mathrm{E_A}\bar{\varepsilon}_t. \quad (20)$$

2. *Forward phase transformation:* $\bar{\varepsilon}_t\in[\bar{\varepsilon}_{\mathrm{AM}}(0),\bar{\varepsilon}_{\mathrm{AM}}(1)]$. *The stress, the strain and the phase transformation variable are linked during the forward phase transformation through the relations*

$$z_t=(\bar{\varepsilon}_{\mathrm{AM}})^{-1}(\bar{\varepsilon}_t),\quad \sigma=\bar{\sigma}_{\mathrm{AM}}(z_t). \quad (21)$$

where the two functions $z\mapsto\bar{\varepsilon}_{\mathrm{AM}}(z)$, $z\mapsto\bar{\sigma}_{\mathrm{AM}}(z)$ *on* $[0,1]$ *are defined as follows*

$$\bar{\sigma}_{\mathrm{AM}}(z)=\frac{\sqrt{\mathrm{p}'(z)^2+2\mathrm{S}'(z)(\mathrm{G}'(z)+\mathrm{R}'(z))}-\mathrm{p}'(z)}{\mathrm{S}'(z)},$$
$$\bar{\varepsilon}_{\mathrm{AM}}(z)=\mathrm{S}(z)\bar{\sigma}_{\mathrm{AM}}(z)+\mathrm{p}(z). \quad (22)$$

3. *Martensite phase:* $\bar{\varepsilon}_t\in[\bar{\varepsilon}_{\mathrm{AM}}(1),+\infty)$. *The response becomes again elastic. The phase transformation variable is equal to 1 and the stress–strain relation reads*

$$\sigma_t=\mathrm{E_M}(\bar{\varepsilon}_t-\mathrm{p}_1). \quad (23)$$

Proposition 4.2 (Homogeneous backward phase transformation). *The response of the material point during the unloading phase* ($t\mapsto\bar{\varepsilon}$ *decreasing) follows three successive stages:*

1. *Martensite phase:* $\bar{\varepsilon}_t\in[\bar{\varepsilon}_{\mathrm{MA}}(1),+\infty)$. *At the onset of the loading, the response of the material is first elastic. The phase transformation variable is equal to 0, while the stress is given by*

$$\sigma_t=\mathrm{E_M}(\bar{\varepsilon}_t-\mathrm{p}_1). \quad (24)$$

2. *Backward phase transformation:* $\bar{\varepsilon}_t\in[\bar{\varepsilon}_{\mathrm{MA}}(0),\bar{\varepsilon}_{\mathrm{MA}}(1)]$. *The stress, the strain and the phase transformation variable are linked during the backward phase transformation through the relations*

$$\bar{\varepsilon}_t=\bar{\varepsilon}_{\mathrm{MA}}(z_t),\quad \sigma=\bar{\sigma}_{\mathrm{MA}}(z_t). \quad (25)$$

where the two functions $z\mapsto\bar{\varepsilon}_{\mathrm{MA}}(z)$, $z\mapsto\bar{\sigma}_{\mathrm{MA}}(z)$ *on* $[0,1]$ *are defined as follows*

$$\bar{\sigma}_{MA}(z) = \frac{\sqrt{p'(z)^2 + 2S'(z)(G'(z) - R'(z))} - p'(z)}{S'(z)},$$
$$\bar{\varepsilon}_{MA}(z) = S(z)\bar{\sigma}_{MA}(z) + p(z), \quad (26)$$

3. *Austenite phase:* $\bar{\varepsilon}_t \in [0, \bar{\varepsilon}_{MA}(0)]$. *The response becomes again elastic. The phase transformation variable is equal to 1, while the stress is given by*

$$\sigma_t = E_A \bar{\varepsilon}_t. \quad (27)$$

Proof. We invite the reader to refer to Pham (2014) for a detailed proof. □

Knowing the intrinsic response of the material, we can now introduce a set of definitions related to the hardening and softening properties of the model:

Definition 4.3 (*Hardening and softening phase transformation behavior*). The forward (*resp.* backward) phase transformation is said to be stress-hardening if $\bar{\sigma}'_{AM}(z) > 0$ (*resp.* $\bar{\sigma}'_{MA}(z) > 0$) and stress-softening if $\bar{\sigma}'_{AM}(z) < 0$ (*resp.* $\bar{\sigma}'_{MA}(z) < 0$) for $z \in [0, 1]$.

We will focus in this article only on stress-softening behavior which is responsible of the main issues such as strain localization and loss of uniqueness and which require the regularization of the model. On the other hand, stress-hardening behavior leads to the well-posedness of the evolution problem and stability of the homogeneous state (Pham, 2014).

4.2. Example

To illustrate the intrinsic properties of the model, we consider a set of material functions that allow the calculation of closed form localized solutions as we will see in Section 5. These laws are derived from the ones introduced by Alessi et al. (2014) in the context of gradient damage models with plasticity. First, let us call $z \mapsto w(z)$ an intermediary function defined over $[0, 1]$ as

$$w(z) = \frac{1 - (1 - (1 - \sqrt{\kappa(1-\eta)})z)^2}{1 - \kappa(1-\eta)}, \quad (28)$$

where κ is a positive parameter. Note that the function w is increasing over $[0, 1]$ with $w(0) = 0$ and $w(1) = 1$ and η is given by

$$\eta = 1 - \frac{E_M}{E_A} \quad (29)$$

with E_A and E_M being the Young's modulus of the austenite and the martensite phases. Hence, we introduce the material functions as follows:

$$\begin{cases} E(z) = E_A \frac{1-(1-\kappa(1-\eta))w(z)}{1+(\kappa-1)w(z)}, \\ p(z) = p_1 \frac{\kappa(1-\eta)w(z)}{1-(1-\kappa(1-\eta))w(z)}, \\ R(z) = R_1 w(z), \\ G(z) = G_1 w(z). \end{cases} \quad (30)$$

Therefore, the local model depends on six material parameters, namely E_A, E_M, κ, p_1, G_1 and R_1. In virtue of the homogeneous response given by Proposition 4.1, a direct calculation shows that $z \mapsto \bar{\sigma}_{AM}(z)$ and $z \mapsto \bar{\sigma}_{MA}(z)$ are given by

$$\bar{\sigma}_{AM}(resp.\bar{\sigma}_{MA})(z) = \frac{p_1 E_A (1-\eta)}{\eta}\left(\sqrt{1 + \frac{2\eta(G_1 + (resp. -)R_1)}{E_A p_1^2 \kappa (1-\eta)^2}}(1 - (1-\kappa(1-\eta))w(z))^2 - 1\right). \quad (31)$$

Since $w' > 0$, the model will exhibit stress-softening during the forward and the backward phase transformation if and only if $0 < \kappa < \frac{1}{1-\eta}$. For $\kappa = \frac{1}{1-\eta}$, the homogeneous phase transformation occurs at constant stress while for $\kappa = 0$, the homogeneous phase transformation occurs at constant strain. Thus, the parameter κ measures the magnitude of the stress-softening. Renormalizing the peak nucleation stress in the work of Hallai and Kyriakides (2013), we propose the following material parameters to approximate the experimental intrinsic curve with our model:

$$E_A = 1.5, \quad E_M = 0.5, \quad \kappa = 2.2, \quad p_1 = 4.6\%, \quad R_1 = 1.15, \quad G_1 = 3. \quad (32)$$

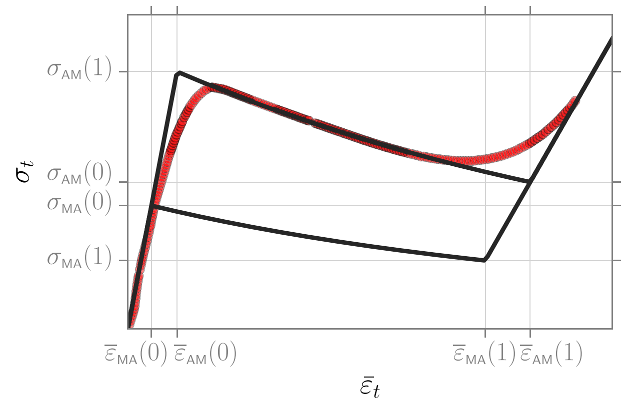

Fig. 1. Intrinsic softening stress–strain curve from our model (Black) versus intrinsic (homogeneous) stress–strain response of NiTi SMA from Hallai and Kyriakides (2013) (Red). (For interpretation of the references to color in this figure legend, the reader is referred to the web version of this article.)

Fig. 1 reports the intrinsic forward and backward response of the model with the above choice of material parameters. Note that in the work of Hallai and Kyriakides (2013), only the intrinsic forward stress–strain curve is obtained through tensile experimental. Indeed, to stabilize a homogeneous evolution, the authors used laminates consisting of face-strips of stainless steel (with a stress-hardening behavior) and NiTi. They showed that such procedure allows to suppress localized evolutions in the NiTi sample. By subtracting the hardening contribution of the stainless steel, they obtained the intrinsic behavior of the NiTi. However, due to the plastic behavior of the stainless steel, the NiTi is constrained to stay in its martensite phase at the end of the experiment and the reverse transformation could not be obtained. As a result, no experimental data could be used for fitting the reverse stress–strain curve. For the sake of completeness, we display in Fig. 1 the analytical results also for the reverse phase transformation. Note that a better fit of the experimental can be obtained with a different set of material functions, see Pham (2014). We choose this model in this paper as it allows for a fully analytical treatment and accounts for the key phenomena revealed in the experiments.

5. Localized evolution

5.1. Evolution of the localized martensite profile

We will first present the construction of a non-homogeneous evolution which will be characterized by three stages: (i) nucleation of a martensite localization; (ii) propagation of the localized phase transformation front; (iii) annihilation of the austenite phase. For each of these three stages, we will derive the phase-field profile in closed-form for the particular constitutive law (28)–(30).

Stage 1: Localized martensite nucleation To construct a localized response, we assume that the non-local phase transformation criterion (14) is reached only on a subset of $(0, L)$ while the remaining part is unloaded elastically. We suppose that the subset where the martensite localization arises at the left end of the bar and is of length Δ_t where Δ_t is a positive parameter which depends in principle on the loading. We will construct here a localized bifurcated branch, starting at the end of the elastic phase when the stress reaches the critical value $\bar{\sigma}_{AM}(0)$. This is the first time instant at which the forward phase transformation criterion becomes an equality over the whole bar:

$$\mathrm{G}'(0)+\mathrm{R}'(0)=\frac{1}{2}\mathrm{S}'(0)\sigma^2_{AM}(0)+\mathrm{p}'(0)\sigma_{AM}(0). \tag{33}$$

Let us call σ_t and $x\mapsto z_t(x)$ the (constant) stress field over the bar and the phase transformation variable associated to the non-homogeneous solution, respectively. On the support $(0,\Delta_t)$ of the half-localization, the forward phase transformation criterion is assumed to be an equality

$$-\mathrm{R}_1\ell^2 z_t''-\frac{1}{2}\mathrm{S}'(z_t)\sigma_t^2-\mathrm{p}'(z_t)\sigma_t+\mathrm{G}'(z_t)+\mathrm{R}'(z_t)=0\quad \text{on}\quad (0,\Delta_t) \tag{34}$$

with the

$$\text{Nucleation boundary conditions}:\begin{cases} z_t'(0)=0,\\ z_t(\Delta_t)=0,\\ z_t'(\Delta_t)=0.\end{cases} \tag{35}$$

The rest of the domain is assumed to be in an austenitic elastic state and hence $z_t=0$ on (Δ_t,L). The phase transformation criterion (14) is then satisfied on (Δ_t,L) provided that $\sigma_t\leqslant\sigma_{AM}(0)$. Now, multiplying (34) by z_t, integrating with respect to x and making use of the boundary conditions (35), we find

$$\frac{1}{2}\mathrm{R}_1\ell^2 z_t'^2=-\frac{1}{2}(\mathrm{S}(z_t)-\mathrm{S_A})\sigma_t^2-\sigma_t\mathrm{p}(z_t)+\mathrm{G}(z_t)+\mathrm{R}(z_t)\quad\text{on}\quad(0,\Delta_t). \tag{36}$$

Now injecting in this first order differential equation the material functions (28)–(30), we obtain

$$\frac{1}{2}\mathrm{R}_1\ell^2 z_t'^2=\mathrm{w}(z_t)\left(\mathrm{G}_1+\mathrm{R}_1-\frac{\frac{1}{2}\kappa\eta\mathrm{S_A}\sigma_t^2}{1-(1-\kappa(1-\eta))\mathrm{w}(z_t)}-\frac{\kappa(1-\eta)\mathrm{p}_1\sigma_t}{1-(1-\kappa(1-\eta))\mathrm{w}(z_t)}\right). \tag{37}$$

By introducing the change of variable

$$x\mapsto\hat{\mathrm{w}}_t(x)=\mathrm{w}(z_t(x)), \tag{38}$$

which is licit since $\mathrm{w}'>0$, after some calculations, Eq. (36) can be rewritten in the form

$$\frac{\mathrm{R}_1\ell^2(1-\kappa(1-\eta))^2}{8(1-\sqrt{\kappa(1-t)})}\hat{\mathrm{w}}_t'^2$$
$$=\hat{\mathrm{w}}_t\left(\frac{1}{2}\kappa\eta\mathrm{S_A}(\sigma_{AM}(0)^2-\sigma_t^2)+\mathrm{p}_1\kappa(1-\eta)(\sigma_{AM}(0)-\sigma_t)\right. \tag{39}$$
$$\left.-(\mathrm{G}_1+\mathrm{R}_1)(1-\kappa(1-\eta))\hat{\mathrm{w}}_t\right), \tag{40}$$

where we used that

$$\mathrm{G}_1+\mathrm{R}_1=\frac{1}{2}\kappa\eta\mathrm{S_A}\sigma^2_{AM}(0)+\kappa(1-\eta)\mathrm{p}_1\sigma_{AM}(0) \tag{41}$$

and the boundary conditions $\hat{\mathrm{w}}_t(0)=0,\ \hat{\mathrm{w}}_t(\Delta_t)=0$. The solution of this differential equation is of the form

$$\hat{\mathrm{w}}_t(x)=\hat{\mathrm{w}}^\star(\sigma_t)\cos^2\left(\frac{\pi x}{2\Delta_{AM}}\right), \tag{42}$$

where Δ_{AM} is given by

$$\Delta_{AM}=\left(\frac{\mathrm{R}_1(1-\kappa(1-\eta))}{8(1-\sqrt{\kappa(1-t)})(\mathrm{G}_1+\mathrm{R}_1)}\right)^{1/2}\pi\ell \tag{43}$$

and $\hat{\mathrm{w}}_t^\star(\sigma_t)$ is defined as

$$\hat{\mathrm{w}}^\star(\sigma_t)=\frac{\frac{1}{2}\kappa\eta\mathrm{S_A}(\sigma_{AM}(0)^2-\sigma_t^2)+\mathrm{p}_1\kappa(1-\eta)(\sigma_{AM}(0)-\sigma_t)}{(\mathrm{G}_1+\mathrm{R}_1)(1-\kappa(1-\eta))} \tag{44}$$

with $\hat{\mathrm{w}}^\star(\sigma_t)\geqslant 0$ for $\sigma_t\leqslant\sigma_{AM}(0)$. Thus, for the present choice constitutive law, the size Δ_{AM} of the localization is constant during the whole nucleation process. Note that the differential equation (40) can be simply rewritten in the form

$$\left(\frac{\Delta_{AM}}{\pi}\right)^2\hat{\mathrm{w}}_t'^2=\hat{\mathrm{w}}_t(\hat{\mathrm{w}}^\star(\sigma_t)-\hat{\mathrm{w}}_t). \tag{45}$$

The localized martensite profile $z_t(x)=\mathrm{w}^{-1}(\hat{\mathrm{w}}_t(x))$ is then obtained by inverting the relation (38) by means of (28). The amplitude of the localization $\hat{\mathrm{w}}^\star(\sigma_t)$ is increasing when σ_t is decreasing with $\hat{\mathrm{w}}^\star(\sigma_{AM}(0))=0$. It reaches the critical value 1 when $\sigma_t=\tilde{\sigma}_{AM}$ where $\tilde{\sigma}_{AM}$ is given by the relation

$$\mathrm{G}_1+\mathrm{R}_1=\frac{1}{2}\frac{\eta}{1-\eta}\tilde{\sigma}^2_{AM}+\mathrm{p}_1\tilde{\sigma}_{AM}. \tag{46}$$

Based on Pham (2014, see Eq. (89)), the stress $\tilde{\sigma}_{AM}$ satisfying the relation (46) precisely corresponds to the forward Maxwell stress[1] of the stress-softening homogeneous phase transformation. We plot in Fig. 2 (Left) the evolution of the half localization for different values of σ_t ranging from $\sigma_{AM}(0)$ to $\tilde{\sigma}_{AM}$.

Stage 2: Propagation of the localized phase transformation front When σ_t reaches the critical Maxwell stress $\tilde{\sigma}_{AM}$, the phase transformation front propagates in the right direction at *fixed* stress. The phase field profile along the bar is reported in Fig. 3. It consists in three different phases:

- $x\in(0,\Theta_t)$: a homogeneous transformed martensitic part of size Θ_t;
- $x\in(\Theta_t,\Theta_t+\Delta_{AM})$: an austenite–martensite mixture part with the same profile than at the end of the previous stage;
- $x\in(\Theta_t+\Delta_{AM},L)$: a homogeneous austenitic part.

To establish how Θ_t evolves with the loading, let us integrate the stress–strain constitutive relation over the bar:

$$\tilde{\sigma}_{AM}\frac{1}{L}\left(\Theta_t\mathrm{S_M}+\int_{\Theta_t}^{\Theta_t+\Delta_{AM}}\mathrm{S}(z_t)dx+(L-\Theta_t-\Delta_{AM})\mathrm{S_A}\right)$$
$$=\bar{\varepsilon}_t-\frac{1}{L}\left(\Theta_t\mathrm{p}_1+\int_{\Theta_t}^{\Theta_t+\Delta_{AM}}\mathrm{p}(z_t)dx\right). \tag{47}$$

We deduce that, during this stage, the length Θ_t grows linearly with the nominal strain $\bar{\varepsilon}_t$ according to the relation

$$\frac{\Theta_t}{L}=\frac{\bar{\varepsilon}_t-\tilde{\bar{\varepsilon}}_{AM}}{(\mathrm{S_M}-\mathrm{S_A})\tilde{\sigma}_{AM}+\mathrm{p}_1}. \tag{48}$$

When $\Theta_t+\Delta_{AM}=L$, the phase transformation front reaches the right end of the bar and the annihilation of the localized phase transformation front begins.

Stage 3: Annihilation of the austenite phase During this stage, the boundary conditions that the phase transformation variable has to satisfy are the following:

$$\text{Annihilation boundary conditions}:\begin{cases} z_t(L-\Delta_{AM})=1,\\ z_t'(L-\Delta_{AM})=0,\\ z_t'(L)=0.\end{cases} \tag{49}$$

Following a similar procedure as for the nucleation phase, by integrating the phase transformation criterion, one can show that the phase field should satisfy the following first order differential equation:

[1] The forward Maxwell stress is the critical height of the horizontal line that cut the *homogeneous* forward stress–strain curve in two separate regions of equal areas.

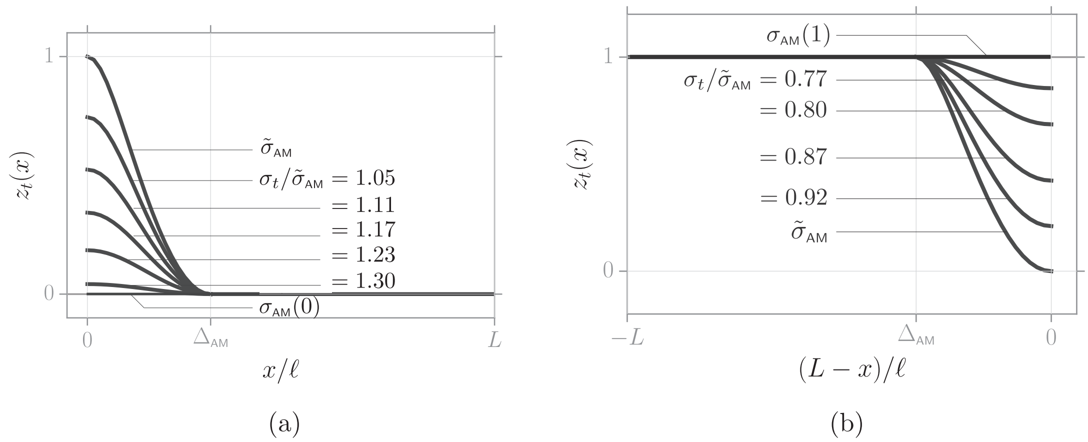

Fig. 2. (Left) Evolution of the martensite front during nucleation phase, σ_t is decreasing from $\sigma_{AM}(0)$ to $\tilde{\sigma}_{AM}$. (Right) Evolution of the martensite front during annihilation phase, σ_t is decreasing from to $\tilde{\sigma}_{AM}$ to $\sigma_{AM}(1)$.

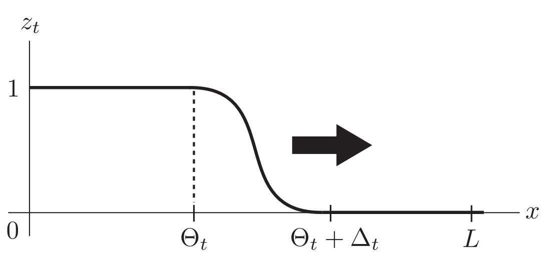

Fig. 3. Propagation of the martensite front phase along the bar.

$$\frac{1}{2}\mathsf{R}_1\ell^2 {z_t'}^2 = -\frac{1}{2}(\mathsf{S}(z_t) - \mathsf{S}_\mathsf{M})\sigma_t^2 - (\mathsf{p}(z_t) - \mathsf{p}_1)\sigma_t + \mathsf{G}(z_t) + \mathsf{R}(z_t) \quad \text{on} \quad (L - \Delta_{AM}, L). \tag{50}$$

For the material law (30), we obtain

$$\frac{1}{2}\mathsf{R}_1\ell^2 {z_t'}^2 = (\mathsf{w}(z_t) - 1) \times \left(\mathsf{G}_1 + \mathsf{R}_1 - \frac{\frac{1}{2}\eta\mathsf{S}_\mathsf{A}\sigma_t^2}{(1-\eta)(1-(1-\kappa(1-\eta))\mathsf{w}(z_t))} - \frac{\mathsf{p}_1\sigma_t}{1-(1-\kappa(1-\eta))\mathsf{w}(z_t)}\right). \tag{51}$$

Using that the critical stress $\sigma_{AM}(1)$ at which the *homogeneous* forward phase transformation ends should satisfy

$$\mathsf{G}_1 + \mathsf{R}_1 = \frac{\frac{1}{2}\kappa\eta\mathsf{S}_\mathsf{A}\sigma_{AM}^2(1)}{\kappa(1-\eta)^2} + \frac{\mathsf{p}_1\sigma_{AM}(1)}{\kappa(1-\eta)}, \tag{52}$$

we find after performing the change of variable (38) that

$$\frac{1}{2}\mathsf{R}_1\ell^2 \frac{(1-\kappa(1-\eta))^2}{4(1-\sqrt{\kappa(1-t)})}\hat{\mathsf{w}}_t'^2 = (\hat{\mathsf{w}}_t - 1)\left(\frac{\frac{1}{2}\kappa\eta\mathsf{S}_\mathsf{A}}{\kappa(1-\eta)}\left(\sigma_{AM}(1)^2 - \kappa(1-\eta)\sigma_t^2\right) + \frac{\mathsf{p}_1}{\kappa(1-\eta)}(\sigma_{AM}(1) - \kappa(1-\eta)\sigma_t) - (\mathsf{G}_1 + \mathsf{R}_1)(1-\kappa(1-\eta))\hat{\mathsf{w}}_t\right). \tag{53}$$

The solution of the such differential equation is of the form

$$\hat{\mathsf{w}}_t(x) = 1 + (\hat{\mathsf{w}}^\circ(\sigma_t) - 1)\cos^2\left(\frac{\pi(L-x)}{2\Delta_{AM}}\right), \tag{54}$$

where $\hat{\mathsf{w}}_t^\circ(\sigma_t)$ is defined as

$$\hat{\mathsf{w}}^\circ(\sigma_t) = \frac{\frac{\frac{1}{2}\kappa\eta\mathsf{S}_\mathsf{A}}{\kappa(1-\eta)}\left(\sigma_{AM}(1)^2 - \kappa(1-\eta)\sigma_t^2\right) + \frac{\mathsf{p}_1}{\kappa(1-\eta)}(\sigma_{AM}(1) - \kappa(1-\eta)\sigma_t)}{(\mathsf{G}_1 + \mathsf{R}_1)(1-\kappa(1-\eta))} \tag{55}$$

with $\hat{\mathsf{w}}^\circ(\sigma_t)$ being strictly increasing from 0 to 1 when σ_t goes from $\tilde{\sigma}_{AM}$ to $\sigma_{AM}(1)$. Here, $\hat{\mathsf{w}}^\circ(\sigma_t)$ corresponds to the minimum value of the localized phase transformation profile at $x = L$. The size of the localization during the annihilation phase is constant and is the same as during the nucleation phase. Note that under such definitions, the differential equation (53) can be simply rewritten as

$$\left(\frac{\Delta_{AM}}{\pi}\right)^2 \hat{\mathsf{w}}_t'^2 = (1 - \hat{\mathsf{w}}_t)(\hat{\mathsf{w}}_t - \hat{\mathsf{w}}^\circ(\sigma_t)). \tag{56}$$

The localized martensite profile $z_t(x)$ is then obtained by inverting the relation (38) by means of (28). We plot in Fig. 2 (Right) the evolution of the annihilation stage for different values of σ_t. When $\sigma_t = \sigma_{AM}(1)$, the bar has completely turned into its martensite phase and the evolution of the bar retrieves its homogeneous elastic character with the martensite Young's modulus.

Remark 1. Once we have established the localized evolution during the forward phase transformation, the reverse localized evolution can be obtained. It suffices to replace R_1 by $-\mathsf{R}_1$ in all the previous calculation in virtue of the form of the reverse phase transformation criterion (15).

5.2. Global stress–strain response

Based on the previous results, we can now derive the global stress–strain response of the bar for the evolution of a phase transformation front. In this perspective, let us integrate over the bar the constitutive relation $\sigma_t = \mathsf{E}(z_t)(\varepsilon_t - \mathsf{p}(z_t))$. Given that σ_t is spatially constant in virtue of the equilibrium, we obtain

$$\sigma_t = \left(\frac{1}{L}\int_0^L \mathsf{S}(z_t)dx\right)^{-1}\left(\bar{\varepsilon}_t - \frac{1}{L}\int_0^L \mathsf{p}(z_t)dx\right). \tag{57}$$

Again, we will distinguish three different cases namely the nucleation, propagation and annihilation stages.

Stage 1: Localized martensite nucleation During this stage, the martensite consists in a half-localization on a part of the bar of length Δ_{AM} while the remaining part is in the austenite phase. Hence, we have

$$\frac{1}{L}\int_0^L \mathsf{S}(z_t)dx = \frac{1}{L}\left(\int_0^{\Delta_{AM}} \mathsf{S}(z_t)dx + (L - \Delta_{AM})\mathsf{S}_\mathsf{A}\right), \tag{58}$$

where the first integral term of the right hand side reads

$$\int_0^{\Delta_{AM}} \mathsf{S}(z_t)dx = \mathsf{S}_\mathsf{A}\int_0^{\Delta_{AM}} \frac{1 + (\kappa - 1)\mathsf{w}(z_t)}{1 - (1 - \kappa(1-\eta))\mathsf{w}(z_t)}dx. \tag{59}$$

Given the differential equation (45) from which is derived the localized martensite profile (42), let us perform the change of variable $y = \cos^2\left(\frac{\pi x}{2\Delta_{AM}}\right)$. This gives

$$\int_0^{\Delta_{AM}} \mathsf{S}(z_t)dx = \frac{\Delta_{AM}\mathsf{S}_A}{\pi}\int_0^1 \frac{1+(\kappa-1)\hat{w}^\star(\sigma_t)y}{(1-(1-\kappa(1-\eta))\hat{w}^\star(\sigma_t)y)\sqrt{y(1-y)}}dy. \tag{60}$$

With the same reasoning, we also have for the integration of the martensitic strain

$$\int_0^L \mathsf{p}(z_t)dx = \frac{\kappa(1-\eta)\Delta_{AM}\mathsf{p}_1}{\pi}\int_0^1 \frac{\hat{w}^\star(\sigma_t)y}{(1-(1-\kappa(1-\eta))\hat{w}^\star(\sigma_t)y)\sqrt{y(1-y)}}dy \tag{61}$$

Therefore, we have obtained the following global stress–strain relation that governs the localized martensite nucleation stage

$$\bar{\varepsilon}_t = \mathsf{S}_A\sigma_t + \frac{\Delta_{AM}}{\pi L}(\kappa\eta\mathsf{S}_A\sigma_t + \kappa(1-\eta)\mathsf{p}_1) \times \int_0^1 \frac{\hat{w}^\star(\sigma_t)\sqrt{y}}{(1-(1-\kappa(1-\eta))\hat{w}^\star(\sigma_t)y)\sqrt{1-y}}dy. \tag{62}$$

Stage 2: Propagation of the localized phase transformation front. This stage occurs at the constant Maxwell stress $\tilde{\sigma}_{AM}$. Let us call $\tilde{\bar{\varepsilon}}_{AM}$ the nominal strain value at which the martensite localization reaches the value 1 *i.e.* when $\sigma_t = \tilde{\sigma}_{AM}$ in (62)

$$\tilde{\bar{\varepsilon}}_{AM} = \frac{1}{L}\left(\int_0^{\Delta_{AM}} \mathsf{S}(z_t)dx + (L-\Delta_{AM})\mathsf{S}_A\right)\tilde{\sigma}_{AM} + \frac{1}{L}\int_0^{\Delta_{AM}} \mathsf{p}(z_t)dx. \tag{63}$$

The propagation starts when the martensite nucleation reaches the value 1 for $\bar{\varepsilon}_t = \tilde{\bar{\varepsilon}}_{AM}$ and ends when the front reaches the right end for $\bar{\varepsilon}_t = \tilde{\bar{\varepsilon}}^*_{AM}$ with

$$\tilde{\bar{\varepsilon}}^*_{AM} = \tilde{\bar{\varepsilon}}_{AM} + \left(1 - \frac{\Delta_{AM}}{L}\right)((\mathsf{S}_M - \mathsf{S}_A)\tilde{\sigma}_{AM} + \mathsf{p}_1 \tag{64}$$

according to (48).

Stage 3: Annihilation of the austenite phase Finally, let us derive the global stress–strain response during the annihilation stage which consist in the disappearance of the half localization at the right end of the bar. Following the same procedure as in the nucleation stage, let us first compute the spacial average of the compliance which reads

$$\frac{1}{L}\int_0^L \mathsf{S}(z_t)dx = \frac{1}{L}\left((L-\Delta_{AM})\mathsf{S}_M + \int_{L-\Delta_{AM}}^L \mathsf{S}(z_t)dx\right). \tag{65}$$

Given the change of variable $y = \cos^2\left(\frac{\pi(L-x)}{2\Delta_{AM}}\right)$ and the differential equation (56), we obtain for the integral over the half-localization

$$\int_{L-\Delta_{AM}}^L \mathsf{S}(z_t)dx = \frac{\Delta_{AM}\mathsf{S}_A}{\pi} \times \int_0^1 \frac{1+(\kappa-1)(1+(1-\hat{w}^\circ(\sigma_t))y)}{(1-(1-\kappa(1-\eta))(1+(1-\hat{w}^\circ(\sigma_t))y))\sqrt{y(1-y)}}dy. \tag{66}$$

On the other hand, the average of the martensitic strain is

$$\frac{1}{L}\int_0^L \mathsf{p}(z_t)dx = \frac{1}{L}\left((L-\Delta_{AM})\mathsf{p}_1 + \int_{L-\Delta_{AM}}^L \mathsf{p}(z_t)dx\right), \tag{67}$$

where $\int_{L-\Delta_{AM}}^L \mathsf{p}(z_t)dx$ is given by

$$\int_{L-\Delta_{AM}}^L \mathsf{p}(z_t)dx = \frac{\Delta_{AM}\mathsf{p}_1}{\pi}\int_0^1 \times \frac{\kappa(1-\eta)\left(\hat{w}^\circ_t(\sigma_t) + (1-\hat{w}^\circ_t(\sigma_t))y\right)}{(1-(1-\kappa(1-\eta))\hat{w}^\circ_t(\sigma_t)y)\sqrt{y(1-y)}}dy. \tag{68}$$

Finally, the global stress–strain relation is again deduced by means of (57). To obtain the reverse global response during the backward transformation, it suffices to replace R_1 by $-\mathsf{R}_1$ in all the previous calculation.

On Fig. 4, we have plotted the global response during a whole cycle for $\ell/L = 0.2$. The global response of such localized evolution highly depends on the magnitude of the ratio ℓ/L. In Fig. 5, we see that for sufficiently large ratio ℓ/L, martensite nucleation is a continuous process with respect to the loading parameter. In particular, the total energy evolves continuously during the whole nucleation stage. On the other hand, for sufficiently small values of ℓ/L, two snap-backs occur: one at the peak elastic stress $\sigma_{AM}(0)$ during the nucleation stage and one at the beginning of the annihilation stage. In both cases, the evolution of the total energy and the phase transformation variable are discontinuous in time jumping from the peak stress to the Maxwell stress. In particular, balance of energy cannot be satisfied as it enforces the total energy to be a continuous function of the loading. A quick calculation shows that a snap-back occurs during the forward transformation at the peak stress $\sigma_{AM}(0)$ as soon as $\frac{d\bar{\varepsilon}_t}{d\sigma_t}(\sigma_{AM}(0)) > 0$. With our family of models, given that $\hat{w}^\star(\sigma_{AM}) = 0$, then

$$\frac{d\bar{\varepsilon}_t}{d\sigma_t}(\sigma_{AM}(0)) = \mathsf{S}_A + \frac{\Delta_{AM}}{2L}(\kappa\eta\mathsf{S}_A\sigma_{AM}(0) + \kappa(1-\eta)\mathsf{p}_1)(\hat{w}^\star)'(\sigma_{AM}(0)). \tag{69}$$

We deduce the critical length L^*_{AM} above which a snap-back occurs

$$L^*_{AM} = \frac{(\kappa\eta\mathsf{S}_A\sigma_{AM}(0) + \kappa(1-\eta)\mathsf{p}_1)^2}{2\mathsf{S}_A\Delta_{AM}(\mathsf{G}_1+\mathsf{R}_1)(1-\kappa(1-\eta))}. \tag{70}$$

5.3. Energy balance condition and time regularity of the evolution

Regularity in time of quasi-static evolutions is an important issue for softening models. Indeed, for bars of length L such that $L > L^*_{AM}$ we have seen that a snap-back in the global response occurs during the localized martensite nucleation. Such snap-back prevents from following continuously the global response with respect to the increasing loading parameter. In particular, by jumping from the peak stress $\sigma_{AM}(0)$ to the Maxwell stress $\tilde{\sigma}_{AM}$, the total energy and the local fields will experience also a time discontinuity, some energy will be lost during the nucleation process and the energy balance condition will not be satisfied. To deal with such issue, different points of views can be adopted.

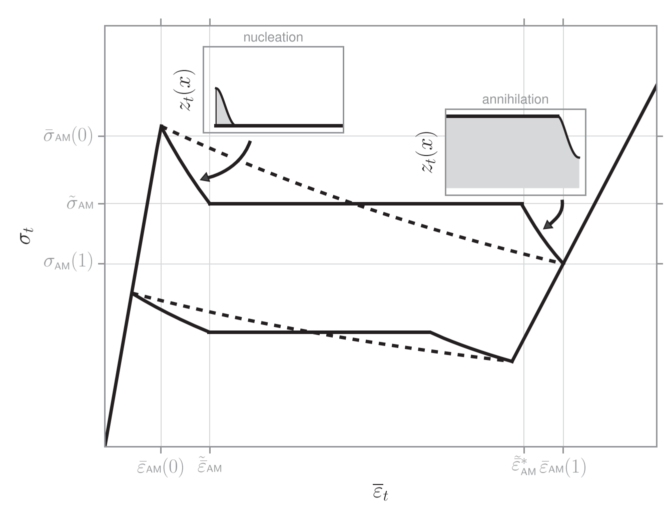

Fig. 4. Global stress–strain diagram of the localized (plain line) and homogeneous (dashed line) phase transformation evolution for $\ell/L = 0.2$. During nucleation, propagation, and annihilation of the martensite front, the spatially constant stress decreases from $\sigma_{AM}(0)$ to $\tilde{\sigma}_{AM}$ and from $\tilde{\sigma}_{AM}$ to $\sigma_{AM}(1)$, respectively.

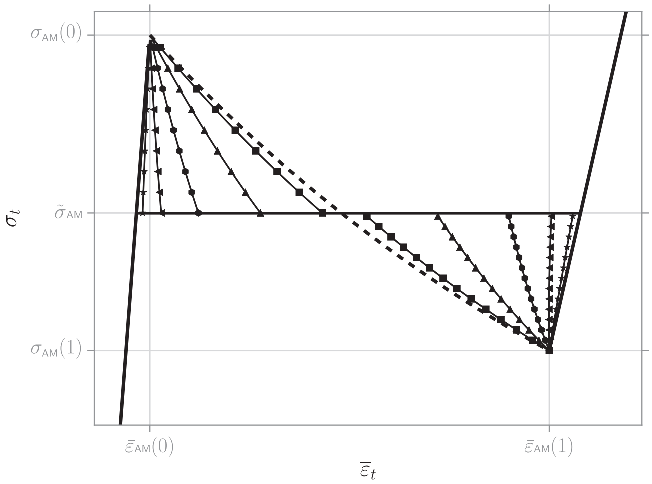

Fig. 5. Influence of the ratio ℓ/L on the forward global response of the localized evolution: the smaller is ℓ/L, the greater is the snap-back. Markers refer to different values of the ratio ℓ/L as follows: ★ : 0.02, ◀ : 0.08, ● : 0.2, ▲ : 0.4, ■ : 0.6, whereas the dashed line corresponds to the homogenous evolution. The insets represent the localized evolution during nucleation and annihilation.

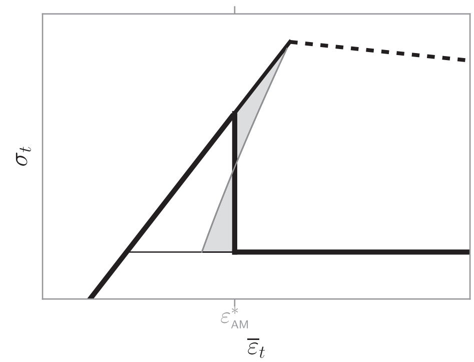

Fig. 6. Evolution path (thick, black line) that satisfies the energy balance condition in case of a snap-back for $\ell/L = 0.02$. The energy-conserving path corresponds to the Maxwell line that equates the two gray areas.

On the one hand, one can assume that such time discontinuity in the global response is a manifestation of the dynamic nature of the nucleation process that is not captured by a quasi-static approach for long bars. The dynamic modeling of such stage would in principle account for the kinetic energy consumed during this stage. However it is a difficult task that goes beyond the scope of the presented framework. On the other hand, if one remains in a pure quasi-static setting, it is still important to evaluate precisely the energy loss through this nucleation process. To achieve such task, one has to be able to follow the snap-back, whether by means of a continuation method or analytically as presented before in this one dimensional context. Then, the energy loss during the nucleation process can be obtained by computing the difference of areas in the global stress–strain diagram when jumping from the peak stress $\sigma_{AM}(0)$ to the Maxwell stress $\tilde{\sigma}_{AM}$. Of course, we cannot assert that this difference of energy corresponds to the kinetic energy that would be obtained in a dynamic approach. Nevertheless it still gives a relevant information on how the quasi-static approach can deal with such discontinuity issue.

Moreover, assuming that the snap-back in the global response is known, an alternative evolution can be proposed. Indeed, one can enforce the energy balance condition to be satisfied, even through the nucleation stage. Since the total energy of the system is given in the global stress–strain response, a possible choice is to follow the vertical line labeled by the critical elongation ε^*_{AM} shown on Fig. 6. Such line is constructed in such a way that the two gray zones are of equal area and thus, corresponds to a vertical Maxwell line associated to the nucleation process. As a result, following this vertical line will ensure the continuity of the total energy and will enforce the energy balance condition. Note that the strain and phase fields will still experience a time discontinuity. Note that as the ratio ℓ/L diminishes, the snap-back becomes more pronounced and thus, the vertical Maxwell line tends to shift towards the critical strain $\tilde{\sigma}_{AM}/E_A$. Despite enforcing the energy balance condition, such approach can be questioned as the austenite elastic stage is stable (Pham, 2014) and leaving such stable would force to cross an energy barrier.

Experiments on NiTi wires give different kind of answers on this issue of nucleation. In particular, depending on how the boundary conditions are applied, martensite nucleation can occur at different stress level. For instance, if no particular precautions are taken at the boundaries, due to the stress concentration, some austenite already transforms into martensite inside the grips at the onset of the loading. In this case, the macroscopic martensite localization tends to occur approximatively at the Maxwell stress level, see for instance Shaw and Kyriakides (1995). On the other hand, Iadicola and Shaw (2002) showed that by increasing locally the temperature where the NiTi is gripped by means of a temperature-controlled conduction block, the austenite is stabilized at the boundaries. In this case, the martensitic transformation appears in the bulk of the specimen where the stress and temperature fields are uniform with a peak nucleation stress significantly higher than the Maxwell stress, see for instance Fig. 9 in Iadicola and Shaw (2002).

6. Conclusions

In this article, we have studied localized evolutions of a superelastic regularized rate-independent SMA model. The total strain energy of the system is defined as the sum of a free energy and a dissipated energy. Regularization is taken of the simplest form by adding quadratic terms of the gradient of the internal variable in the free energy. This results in a model that depends on four material functions of the internal variable along with an internal length ℓ. The quasi-static evolution problem of one dimensional bar of length L is formulated in terms of two physical principles: a stability criterion (**S**) which enforces at each time step local minimality of the total energy among a space of admissible states and an energy balance condition (**E**) which requires the absolute continuity of the total energy of the system with respect to the loading parameter. By writing the first order condition of stability, we derive the local equations, namely the bar equilibrium, the nonlocal Kuhn–Tucker conditions as well as natural boundary conditions associated to the phase transformation.

Localized evolutions of the phase transformation have been fully investigated for a specific class of material functions, from the onset of the martensitic phase transformation to the backward transformation. Closed-form formula of the localized phase transformation profile have been derived as well as the associated global responses. Those responses are strongly dependent of the length ratio ℓ/L. Specifically, for $L > L^*_{AM}$, the martensite nucleation is a continuous process at both local *i.e.* localization profile, and global level *i.e.* total energy. For $L < L^*_{AM}$, the presence of a snap-back requires to reconsider the evolution to satisfy the energy balance condition. A possibility is to follow the vertical Maxwell line related to the snap-back. In this case, although at the local level the nucleation remains a brutal event, the continuity of the total energy is retrieved. Future works will be dedicated to a generalization of such energetic approach in a higher dimensional case and non-proportional loadings.

Appendix A

Proof of Proposition 3.1. By putting $\beta = 0$ in (13), we obtain the weak form of the mechanical equilibrium

$$\forall v \in \mathcal{C}_0, \quad \int_0^L \sigma_t v' dx = 0, \tag{71}$$

where $\sigma_t = \frac{\partial \phi}{\partial \varepsilon}(u'_t, z_t) = \mathsf{E}(z_t)(u'_t - \mathsf{p}(z_t))$ corresponds to the stress field in the bar. Integrating by part (71), we find

$$-\int_0^L \sigma'_t v dx + [\sigma_t v]_0^L = 0. \tag{72}$$

Since $v \in \mathcal{C}_0$, we have $v(0) = v(L) = 0$. By a classical argument of calculus of variation, we deduce that the stress σ_t is spatially constant and only depends on time t. Now by putting $v = 0$ in (13), we obtain the weak form of the phase transformation criterion. Integrating it by parts, we find

$$\int_0^L \left(\frac{\partial \phi}{\partial z}(u'_t, z_t)\beta - \mathsf{R}_1 \ell^2 z''_t \beta + \mathsf{R}'(z_t)|\beta|\right) dx - [\mathsf{R}_1 \ell^2 z'_t \beta]_0^L \geqslant 0. \tag{73}$$

Let us first consider test direction $\beta \in \mathcal{Z}(z_t)$ such that $\beta \geqslant 0$ on $(0, L)$ and $\beta(0) = \beta(L) = 0$. On the subsets of $(0, L)$ where $z_t = 1$, we have necessarily $\beta = 0$. Then, (73) reduces to

$$\forall \beta \geqslant 0, \quad \int_{z_t<1} \left(\frac{\partial \phi}{\partial z}(u'_t, z_t) - \mathsf{R}_1 \ell^2 z''_t + \mathsf{R}'(z_t)\right)|\beta| dx \geqslant 0. \tag{74}$$

Again, by means of a classical argument of calculus of variation, we find that

$$\frac{\partial \phi}{\partial z}(u'_t, z_t) - \mathsf{R}_1 \ell^2 z''_t + \mathsf{R}'(z_t) \geqslant 0 \quad \text{where} \quad z_t < 1. \tag{75}$$

Conversely, let us consider test direction $\beta \in \mathcal{Z}(z_t)$ such that $\beta \leqslant 0$ on $(0, L)$ and $\beta(0) = \beta(L) = 0$. On the subsets of $(0, L)$ where $z_t = 0$, we have necessarily $\beta = 0$. Then, (73) reduces to

$$\forall \beta \geqslant 0, \quad \int_{z_t>0} \left(-\frac{\partial \phi}{\partial z}(u'_t, z_t) + \mathsf{R}_1 \ell^2 z''_t + \mathsf{R}'(z_t)\right)|\beta| dx \geqslant 0. \tag{76}$$

Again, using a classical argument of calculus of variation, we find that

$$-\frac{\partial \phi}{\partial z}(u'_t, z_t) + \mathsf{R}_1 \ell^2 z''_t + \mathsf{R}'(z_t) \geqslant 0 \quad \text{where} \quad z_t > 0. \tag{77}$$

Non-local inequalities (75) and (77) constitute the phase transformation criteria that rule the forward and backward phase transformations, respectively. In particular, the non-local Laplacian term of z_t is not introduced arbitrarily but is instead derived naturally from the first order optimality condition. It remains to derive the boundary conditions on the phase transformation variable. Again, this is done from the weak form of the phase transformation criterion (73). By considering vanishing β in the bulk but which remain non-zero at the boundaries, we find in the limit that

$$-\mathsf{R}_1 \ell^2 z'_t(L)\beta(L) + \mathsf{R}_1 \ell^2 z'_t(0)\beta(0) \geqslant 0 \tag{78}$$

for any $\beta \in \mathcal{Z}(z_t)$. We then deduce the following boundary conditions at $x = 0$

$$\begin{cases} z'_t(0) \geqslant 0 & \text{if} \quad z_t(0) < 1; \\ z'_t(0) \leqslant 0 & \text{if} \quad z_t(0) > 0 \end{cases} \tag{79}$$

and at $x = L$

$$\begin{cases} z'_t(L) \leqslant 0 & \text{if} \quad z_t(L) < 1; \\ z'_t(L) \geqslant 0 & \text{if} \quad z_t(L) > 0. \end{cases} \quad \square \tag{80}$$

Proof of Proposition 3.2. By taking the right derivating of the energy balance condition (10) with respect to time, we find

$$\int_0^L \left(\frac{\partial \phi}{\partial \varepsilon}(u'_t, z_t)\dot{u}'_t + \frac{\partial \phi}{\partial z}(u'_t, z_t)\dot{z}_t + \mathsf{R}_1 \ell^2 z'_t \dot{z}'_t\right) dx + \int_0^L \mathsf{R}'(z_t)|\dot{z}_t| dx = \sigma_t \dot{U}_t. \tag{81}$$

Integrating by parts the last term of the first integral and making use of the equilibrium which gives

$$\int_0^L \left(\frac{\partial \phi}{\partial \varepsilon}(u'_t, z_t)\dot{u}'_t\right) dx = \sigma_t \int_0^L \dot{u}'_t dx = \sigma_t \dot{U}_t,$$

we obtain

$$\int_0^L \left(\frac{\partial \phi}{\partial z}(u'_t, z_t) - \mathsf{R}_1 \ell^2 z''_t\right)\dot{z}_t dx - [\mathsf{R}_1 \ell^2 z'_t \dot{z}_t]_0^L + \int_0^L \mathsf{R}'(z_t) \mid \dot{z}_t \mid dx = 0. \tag{82}$$

By considering now the subsets of $[0, L]$ where $\dot{z}_t > 0$ and $\dot{z}_t < 0$, let us decompose (82) as

$$\begin{aligned} &\int_{|\dot{z}_t|>0} \left(\frac{\partial \phi}{\partial z}(u'_t, z_t) + \mathsf{R}'(z_t) - \mathsf{R}_1 \ell^2 z''_t\right)|\dot{z}_t| dx \\ &+ \int_{|\dot{z}_t|<0} \left(\frac{\partial \phi}{\partial z}(u'_t, z_t) - \mathsf{R}'(z_t) - \mathsf{R}_1 \ell^2 z''_t\right)|\dot{z}_t| dx \\ &- \mathsf{R}_1 \ell^2 z'_t(L)\dot{z}_t(L) + \mathsf{R}_1 \ell^2 z'_t(0)\dot{z}_t(0) = 0 \end{aligned} \tag{83}$$

Since $z_t < 1$ (resp. $z_t > 0$) when $\dot{z}_t > 0$ (resp. $\dot{z}_t < 0$) and given (79) and (80), we deduce that all the terms of the left-hand side of (83) are positive. As a result, we have found the following consistency conditions in the bulk

$$\mathsf{R}'(z_t)\dot{z}_t = \left(-\frac{\partial \phi}{\partial z}(u'_t, z_t) + \mathsf{R}_1 \ell^2 z''_t\right)|\dot{z}_t| \tag{84}$$

and at the boundaries

$$z'_t(L)\dot{z}_t(L) = 0, \quad z'_t(0)\dot{z}_t(0) = 0. \quad \square \tag{85}$$

References

Alessi, R., Marigo, J.-J., Vidoli, S., 2014. Gradient damage models coupled with plasticity: variational formulation and main properties. Mech. Mater. http://dx.doi.org/10.1016/j.mechmat.2013.12.005.

Auricchio, F., Sacco, E., 1997. A one-dimensional model for superelastic shape-memory alloys with different elastic properties between austenite and martensite. Int. J. Non-Linear Mech. 32 (6), 1101–1114.

Ball, J.M., James, R.D., 1989. Fine phase mixtures as minimizers of energy. In: Analysis and Continuum Mechanics. Springer, Berlin Heidelberg, pp. 647–686.

Bazant, Z., Pijaudier-Cabot, G., 1989. Measurement of characteristic length of nonlocal continuum. J. Eng. Mech. ASCE 115 (4), 755–767.

Bhattacharya, K., 2003. Microstructure of Martensite: Why It forms and How It gives Rise to the Shape-Memory Effect, vol. 2. Oxford University Press.

Bourdin, B., Francfort, G.A., Marigo, J.-J., 2008. The variational approach to fracture. J. Elast. 91 (1–3), 5–148.

Carr, J., Gurtin, M.E., Slemrod, M., 1985. One-dimensional structured phase transformations under prescribed loads. J. Elast. 15 (2), 133–142.

Cherkaoui, M., Berveiller, M., Sabar, H., 1998. Micromechanical modeling of martensitic transformation induced plasticity (trip) in austenitic single crystals. Int. J. Plast. 14 (7), 597–626.

Duval, A., Haboussi, M., Ben Zineb, T., 2011. Modelling of localization and propagation of phase transformation in superelastic SMA by a gradient nonlocal approach. Int. J. Solids Struct. 48 (13), 1879–1893.

Ericksen, J.L., 1975. Equilibrium of bars. J. Elast. 5 (3), 191–201.

Frémond, M., Nedjar, B., 1996. Damage, gradient of damage and principle of virtual power. Int. J. Solids Struct. 33 (8), 1083–1103.

Friedman, A., Sprekels, J., 1990. Steady states of austenitic–martensitic domains in the Ginzburg–Landau theory of shape memory alloys. Continuum Mech. Thermodyn. 2 (3), 199–213.

Gurtin, M.E., Anand, L., 2005. A theory of strain-gradient plasticity for isotropic, plastically irrotational materials. Part I: Small deformations. J. Mech. Phys. Solids 53 (7), 1624–1649.

Hallai, J.F., Kyriakides, S., 2013. Underlying material response for lüders like instabilities. Int. J. Plast. 47, 1–12.

Halphen, B., Nguyen, Q.S., 1975. Sur les matériaux standard généralisés. J. Mec. 14, 39–63.

Huo, Y., Müller, I., 1993. Nonequilibrium thermodynamics of pseudoelasticity. Continuum Mech. Thermodyn. 5 (3), 163–204.

Iadicola, M.A., Shaw, J.A., 2002. An experimental setup for measuring unstable thermo-mechanical behavior of shape memory alloy wire. J. Intell. Mater. Syst. Struct. 13 (2-3), 157–166.

Mielke, A., 2005. Evolution of rate-independent systems. In: Evolutionary equations. Handbook of Differential Equations, vol. II. Elsevier/North-Holland, Amsterdam, pp. 461–559.

Pham, K., 2014. An energetic formulation of a one-dimensional model of superelastic shape memory alloys. Continuum Mech. Thermodyn. http://dx.doi.org/10.1007/s00161-014-0346-9.

Pham, K., Marigo, J.-J., Maurini, C., 2011. The issues of the uniqueness and the stability of the homogeneous response in uniaxial tests with gradient damage models. J. Mech. Phys. Solids 59 (6), 1163–1190.

Popov, P., Lagoudas, D.C., 2007. A 3-d constitutive model for shape memory alloys incorporating pseudoelasticity and detwinning of self-accommodated martensite. Int. J. Plast. 23 (10), 1679–1720.

Puglisi, G., Truskinovsky, L., 2000. Mechanics of a discrete chain with bi-stable elements. J. Mech. Phys. Solids 48 (1), 1–27.

Qiao, Lei, Rimoli, Julian J., Chen, Ying, Schuh, Christopher A., Radovitzky, Raul, 2011. Nonlocal superelastic model of size-dependent hardening and dissipation in single crystal Cu–Al–Ni shape memory alloys. Phys. Rev. Lett. 106, 085504.

Ren, X., Truskinovsky, L., 2000. Finite scale microstructures in nonlocal elasticity. In: Carlson, D.E., Chen, Y. (Eds.), Advances in Continuum Mechanics and Thermodynamics of Material Behavior. Springer, Netherlands, pp. 319–355.

Shaw, J.A., 2002. A thermomechanical model for a 1-d shape memory alloy wire with propagating instabilities. Int. J. Solids Struct. 39 (5), 1275–1305.

Shaw, J.A., Kyriakides, S., 1995. Thermomechanical aspects of NiTi. J. Mech. Phys. Solids 43 (8), 1243–1281.

Shaw, J.A., Kyriakides, S., 1997. On the nucleation and propagation of phase transformation fronts in a NiTi alloy. Acta Mater. 45 (2), 683–700.

Song, Z., Dai, H.H., Sun, Q.P., 2012. Propagation stresses in phase transitions of an SMA wire: new analytical formulas based on an internal-variable model. Int. J. Plast.

Sun, Q.P., Hwang, K.C., 1993a. Micromechanics modelling for the constitutive behavior of polycrystalline shape memory alloys – I. Derivation of general relations. J. Mech. Phys. Solids 41 (1), 1–17.

Sun, Q.P., Hwang, K.C., 1993b. Micromechanics modelling for the constitutive behavior of polycrystalline shape memory alloys – II. Study of the individual phenomena. J. Mech. Phys. Solids 41 (1), 19–33.

Tobushi, H., Tanaka, K., Hori, T., Sawada, T., Hattori, T., 1993. Pseudoelasticity of TiNi shape memory alloy: dependence on maximum strain and temperature. JSME Int. J. Ser. A Mech. Mater. Eng., 09148809 36 (3), 314–318.

Zaki, W., Moumni, Z., 2007. A three-dimensional model of the thermomechanical behavior of shape memory alloys. J. Mech. Phys. Solids 55 (11), 2455–2490.